Turkish Journal of Civil Engineering, 2025, 53-73, Paper 820, ***Research Article***

Calibration of Barcelona Basic Model parameters for Unsaturated Ankara Clay

Maham BASHARAT[1*]
Nabi Kartal TOKER[2]

ABSTRACT

This paper deals with the calibration of the Barcelona Basic Model for intact samples of unsaturated Ankara Clay. Ankara Clay is a stiff to very stiff high-plasticity expansive clay that often contains fissures in its intact form. Intact samples were extracted from the premises of Middle East Technical University in Ankara. A comprehensive experimental campaign was carried out in order to determine the hydraulic and mechanical properties of the sample, encompassing saturated and unsaturated triaxial and oedometric compression tests. Soil Water Retention Curve (SWRC) and shrinkage curve were also determined experimentally. Results of the experiments shed light on the strength characteristics of intact Ankara Clay. These results were further used to calibrate the Barcelona Basic Model such that it could model the unsaturated behavior of the sample under compression and shear loadings. Valuable insights were gained regarding the suitability and feasibility of using the Barcelona Basic Model for Ankara Clay and other similar stiff high-plasticity clays. It was concluded that the Barcelona Basic Model cannot accurately model the behavior of stiff high-plasticity expansive clays such as Ankara Clay because it fails to capture the brittle behavior they tend to exhibit at high suctions.

Keywords: Barcelona basic model, unsaturated clay, stiff clay, constitutive model.

1. INTRODUCTION

Alonso et al. [1] are credited with developing one of the earliest constitutive models that attempts to capture the stress-strain behavior of partially saturated low to moderate expansive soils. It is commonly known as the Barcelona Basic Model (BBM). The BBM was developed as a framework for modelling and predicting the behavior of unsaturated soils. To accomplish this, experimental testing is carried out on soil samples and geotechnical properties of the

Note:
- This paper was received on October 23, 2024 and accepted for publication by the Editorial Board on June 13, 2025.
- Discussions on this paper will be accepted by January 31, 2026.
- https://doi.org/10.18400/tjce.1570696

1 Middle East Technical University, Department of Civil Engineering, Ankara, Türkiye
mahambasharat99@gmail.com - https://orcid.org/0009-0006-9937-7327

2 Middle East Technical University, Department of Civil Engineering, Ankara, Türkiye
toker@metu.edu.tr - https://orcid.org/0000-0001-8858-0510

* Corresponding author

soil are determined. Using these properties, the BBM framework is adjusted and calibrated such that it can accurately model and predict the behavior of that soil. This technique allows researchers and engineers to be able to predict the mechanical behavior of unsaturated soils under a variety of conditions and loadings while reducing their reliance on experimentation.

As mentioned previously, unsaturated soil behavior is commonly determined through experimentation. However, unsaturated soil testing can be a lengthy and costly procedure, requiring sophisticated equipment and long durations, thus rendering these tests impractical for use in most cases. Recently, efforts have been made to simplify testing protocols and develop more practical test procedures [2]. These tests make use of less sophisticated equipment that is easily found in laboratory settings and are also quicker than typical unsaturated soil tests. Furthermore, the results of these tests have also been used to calibrate unsaturated soil constitutive models. This reduces the need for further testing, as soil behavior under various loadings can then be predicted using the calibrated model.

However, previous work in this regard relies on reconstituted or compacted soil samples [2] [3]. Studies have shown that the behavior of soils can be very different in their in-situ state as compared to that of reconstituted samples. Therefore, there is a need to carry out these practical test procedures on intact samples obtained from the field in order to verify whether these procedures can be implemented on the available sample types in the field.

This study attempts to cover the aforementioned gap in the literature. Intact samples of Ankara Clay were collected from within the premises of the Middle East Technical University. Basic tests were carried out on the samples in order to discern its properties and classify the soil type. Since the soil was unsaturated and expansive in nature, the soil water retention curve (SWRC) and shrinkage curve were determined. Saturated and unsaturated triaxial and oedometric compression tests were carried out at various initial moisture contents. Finally, calibration of the Barcelona Basic Model (BBM) was attempted using the results of the aforementioned tests.

2. BACKGROUND

BBM has been developed within the framework of hardening plasticity and as an extension of the Modified Cam Clay (MCC) model. It utilizes two independent stress state variables to model the behavior of soil: net stress (p) and matric suction (s). Net stress is the total stress minus air pressure. Matric suction is the air pressure minus water pressure. The BBM makes use of the Loading-Collapse (LC) and suction increase (SI) yield surfaces to model the behavior of soil (see Figure 1).

Under isotropic conditions, the specific volume of soils is defined as:

$$v = 1 + e = N(s) - \lambda(s)\ln(\frac{p}{p^c}) \quad (1)$$

where p_c is a reference stress, $\lambda(s)$ is the slope of the virgin compression line under constant suction s, and $N(s)$ is the value of specific volume corresponding to the extension of the virgin compression line with a slope of $\lambda(s)$ to reference net stress. N(s) is defined as:

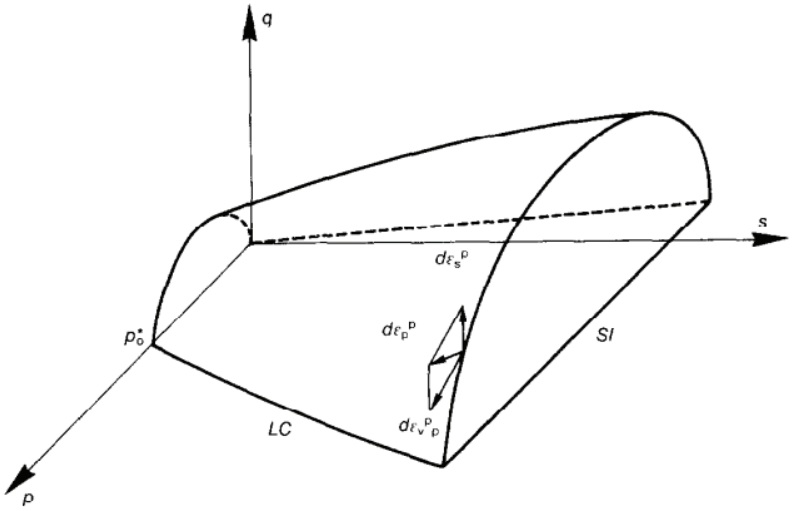

Figure 1 - Yield surface of BBM [1]

$$N(s) = N(0) - \kappa_s \ln\left(\frac{s+p_{atm}}{p_{atm}}\right) \quad (2)$$

where *N(0)* is the specific volume at reference stress for the virgin saturated compression line κ_s is the slope of the elastic compression line due to suction change, p_{atm} is atmospheric pressure

The shape of the LC yield surface is governed by the following equation under isotropic conditions:

$$p_0 = p_c\left(\frac{p_0^*}{p_c}\right)^{\frac{\lambda(s)-\kappa}{\lambda(0)-\kappa}} \quad (3)$$

where $\lambda(0)$ is the slope of the saturated virgin compression line and p_0^* is pre-consolidation stress for saturated condition. $\lambda(s)$ is defined as:

$$\lambda(s) = \lambda(0)[(1-r)\exp(-\beta s) + r] \quad (4)$$

where β controls the rate of increase of soil stiffness with suction, and r is a ratio of the asymptotic value of compression index as suction tends to infinity to saturated compression index λ(0). Practically, r is taken as the ratio of the value of the compression index at the highest suction to the value of the compression index in the saturated state. It is expressed as:

$$r = \frac{\lambda(\infty)}{\lambda(0)} = \frac{Cr(\infty)}{Cr(0)} \quad (5)$$

where C_r is the recompression index.

For the triaxial or deviatoric stress state, the yield curve is an ellipse in the p-q plane, similar to the MCC model. This ellipse expands with an increase in suction due to an increase in cohesion and apparent pre-consolidation pressure which contributes to an increase in shear strength:

$$f = q^2 - M^2(p + ks)(p_0 - p) \tag{6}$$

where M is the slope of the critical state line, k is the parameter controlling the increase in cohesion with suction and s is the suction.

The flow rule defines the ratio of plastic shear strains to plastic volumetric strains:

$$\frac{d\varepsilon_s^p}{d\varepsilon_v^p} = \frac{2q\alpha}{M^2(2p-ks-p_0)} \tag{7}$$

where α is the parameter used to define associated or non-associated flow rule.

3. SOIL CHARACTERIZATION

As mentioned previously, intact samples of Ankara Clay were collected from within the campus of the Middle East Technical University for this study. Samples were collected in a total of sixteen Shelby tubes from four points within a $1m^2$ area. Depth of sample collection ranged from three to five meters. Since all samples were extracted from points in close proximity to each other, they were assumed to be identical and any meso-scale heterogeneities that may have been present were ignored for the purpose of this study. It is also important to note here that Ankara Clay is known for being a fissured, high-plasticity clay [4] [5]. The samples in this study also contained fissures which made intact specimen preparation difficult.

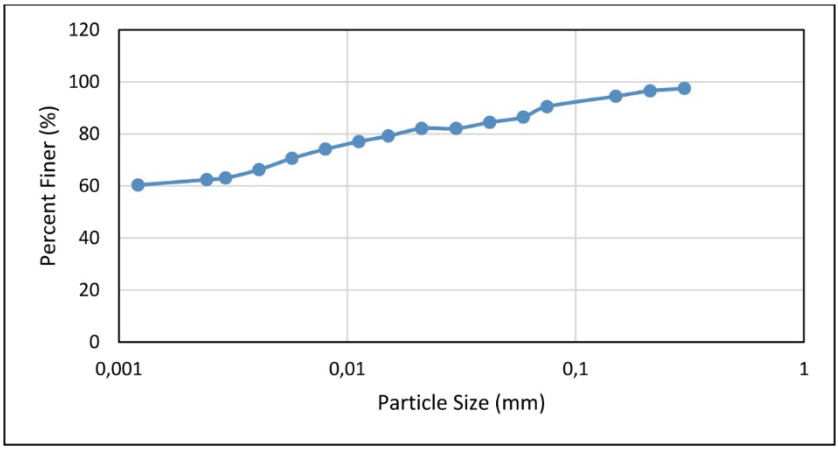

Figure 2 - Particle size distribution of both samples

Index tests were carried out on the specimenin order to determine its basic properties and classify the soil. Particle size distribution was determined through a combination of dry sieving, wet sieving and hydrometer test (see Figure 2).

Specific gravity and Atterberg limits were determined as shown in Table 1. Further index properties as well as some other geotechnical properties (plasticity index (PI), activity, swell potential) were inferred from the results of those tests. Finally, soil classification was done according to USCS.

Table 1 - Summary of Sample Properties

Soil Property	Value
Gs	2.51
LL	81.8
PL	27.1
PI	54.7
Moisture Content	28-33%
% Clay	57.9
% Silt	32.6
% Sand	7.5
% Gravel	2
Activity	0.945
Swell Potential	High
Soil Class	High Plasticity Clay

4. HYDRAULIC PROPERTIES

4.1. Shrinkage Curve

The shrinkage curve was determined by air drying specimens to varying degrees and then measuring their moisture content and bulk density. Void ratio was then calculated from bulk density, moisture content, and specific gravity. Void ratio versus gravimetric moisture content graph was plotted (see Figure 3). The equation of Fredlund et al. [6] was fitted to the data:

$$e(w) = a\left(\left(\frac{w}{b}\right)^{c} + 1\right)^{1/c} \tag{8}$$

where w is the gravimetric water content and a, b and c are constants which were determined as 0.322, 0.130 and 30.268 respectively.

A similar procedure was repeated for the wetting shrinkage curve where specimens were fully dried and then wetted to varying degrees. This allowed for the hysteresis in the shrinkage curve to be captured.

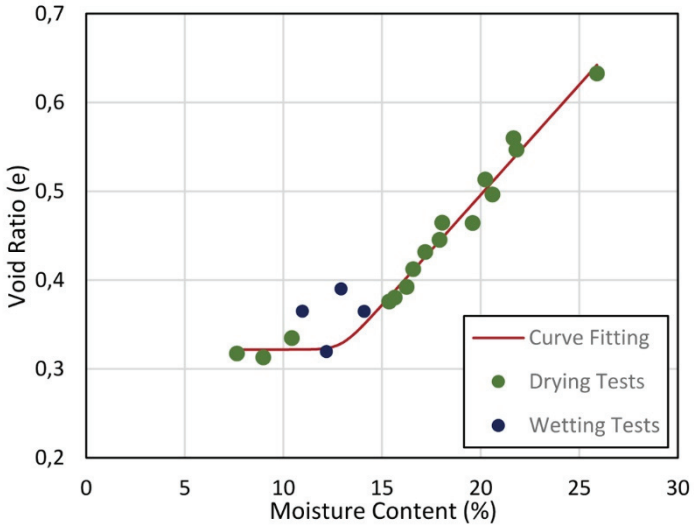

Figure 3 - Shrinkage curve for the intact sample

4.2. Soil Water Retention Curve

Soil Water Retention Curve (SWRC) was determined through a combination of axis translation and vapor equilibrium. Using the former, a suction up to 900 kPa was applied whereas the latter allowed for the imposition of suction up to 91000 kPa. Details regarding SWRC determination can be found in [7].

Figure 4 (a) and (b) display the retention curve in terms of volumetric moisture content and degree of saturation, respectively. It can be seen that the air-entry value of suction is 38000 kPa which corresponds to a gravimetric water content of 13% and a volumetric water content of 25%.

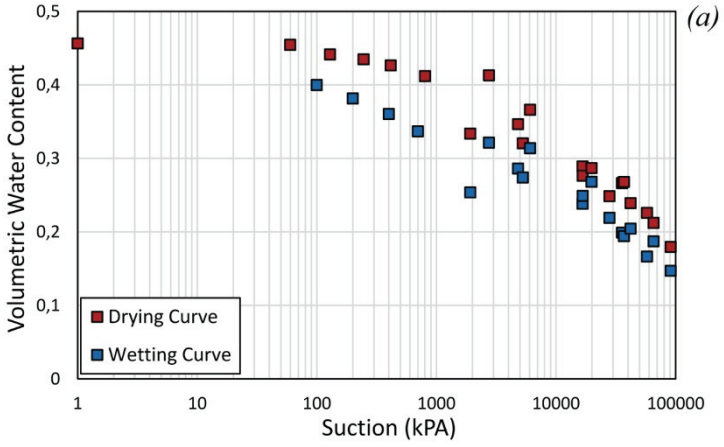

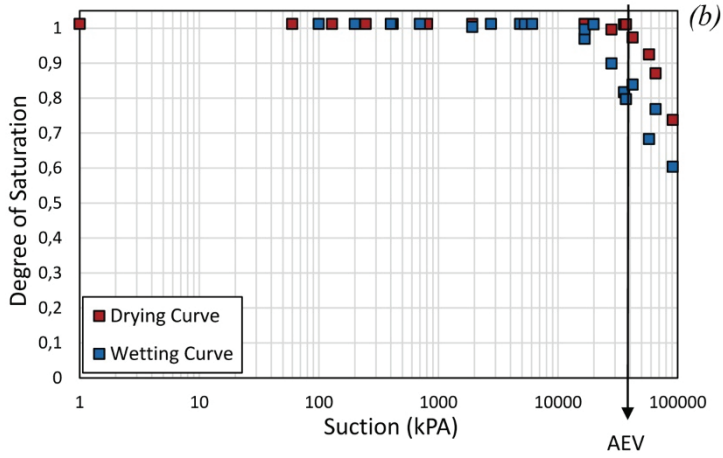

Figure 4 - Soil water retention curve of the sample in terms of (a) volumetric water content, and (b) degree of saturation

The equation developed by [8] was then fit to the SWRC data:

$$\theta = \theta_{res} + \frac{\theta_{sat} - \theta_{res}}{(1+(\frac{s}{s_{aev}})^n)^m} \quad (9)$$

where θ is the volumetric water content, θ_{sat} is the saturated volumetric water content, θ_{res} is the residual volumetric water content, s is the suction, s_{aev} is the air-entry value of the suction, and n and m are fitting parameters.

38000 kPa was used for s_{aev} and the value of θ_{sat} was kept as 45.6%. Ideally, the value of θ_{res} would also be obtained from the experimental data. However, for this soil sample, it was not possible. Therefore, θ_{res} was also kept as a fitting parameter along with m and n.

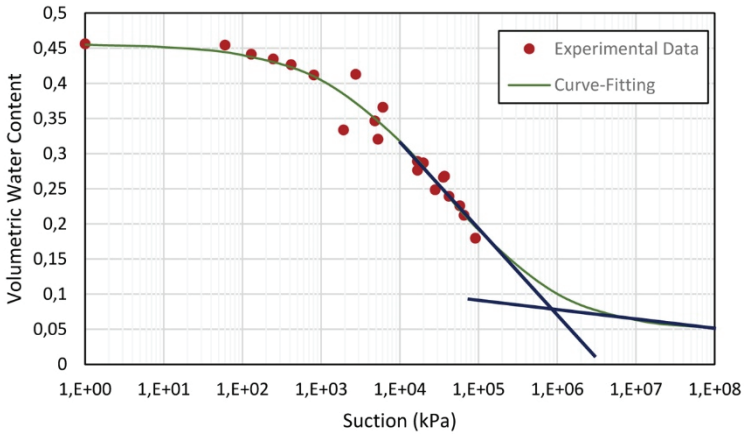

Figure 5 - SWRC developed after curve-fitting

Curve fitting was carried out, minimizing the root mean square error on θ, using the drying curve data and the values of θ_{res}, n and m were determined as 0.047, 0.55 and 1.05. Figure 5 displays the results of the curve-fitting.

5. MECHANICAL PROPERTIES

5.1. Consolidation Test

Consolidation test was carried out on a 1-day soaked specimen in accordance with ASTM D2435 and the loading schedule used was 1-69-139-277-554-693-554-277-554-693-1247 kPa. The results of this test can be seen in Figure 6. From this graph, soil properties were calculated as pre-consolidation pressure (180 kPa), compression index (0.092) and swelling index (0.018). The overburden pressure was calculated as 50 kPa and, consequently the over-consolidation ratio (OCR) was calculated as 3.6.

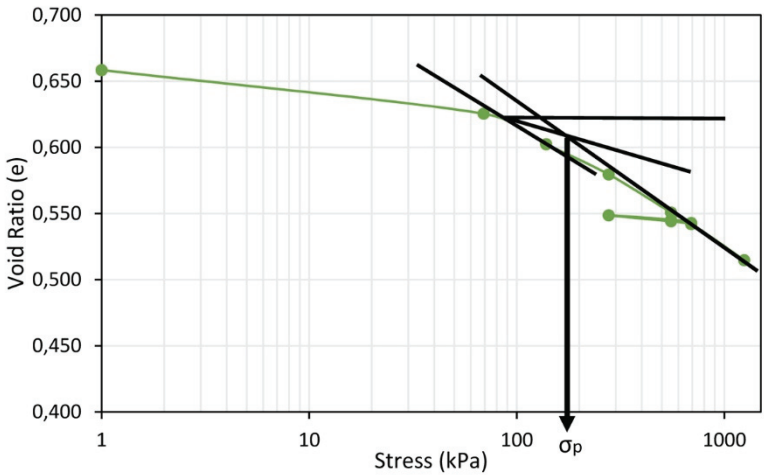

Figure 6 - Compression curve

5.2. CD Triaxial Tests

Conventional saturated CD triaxial tests were carried out in accordance with ASTM D7181 on the specimens at 100 and 400 kPa effective confining pressure using isotropic consolidation. The number of triaxial tests and values of the confining pressures were selected following the procedures of [2]. The strain rate for shearing was determined using the method of [9] and based on the assumption that failure would occur at 8% strain. However, prior to starting the tests, the specimens had to be soaked in a water bath to saturate them and eliminate the high amounts of suction present in the soil naturally. Once specimens were placed in the triaxial test setup, the saturation was checked by checking the Skempton's B-value and, in both cases, it was recored as 0.95, thereby signaling adequate saturation.

Mohr's circles and strength envelope for this sample were plotted (see Figure 7). The value of c' was calculated as -18.25 kPa and ϕ' as 28.72°. The negative value of cohesion can likely be attributed to fissures that might have been present inside the specimens in their in-situ state which likely affect the behavior of the specimen during shearing. The slope of the critical state line (M) was also determined from the mean stress-deviator stress space as 1.14 (see Figure 8). It is important to note here that, ideally, for the calculation of these parameters with least amount of error, there should be three or more Mohr's circles in order to have better accuracy. However, the current study had a limited amount of soil sample available for a large number of tests, thereby forcing the authors to limit the number of repeated tests they could conduct.

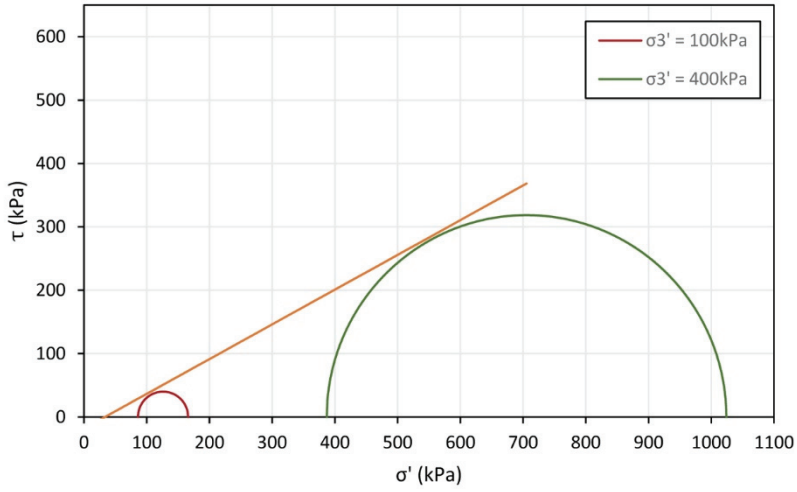

Figure 7 - Mohr's circles and strength envelope from CD triaxial tests

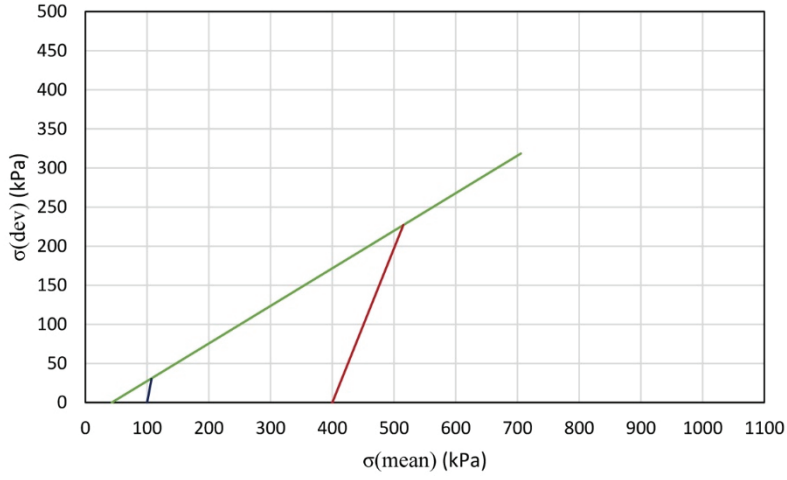

Figure 8 - Deviator stress versus mean stress plot

5.3. Unsaturated Oedometric Compression Tests

Unsaturated oedometric tests were carried out on three specimens at various gravimetric moisture contents-i.e. 10%, 18% and 28%. The procedure followed was the same as the standard oedometer minus the soaking of the specimen. Furthermore, the oedometer cells were covered with plastic wrap in order to prevent moisture loss. Drainage of water out of the specimen was further restricted by using dry filter paper and porous stones. Compression curves were then plotted for all three specimens (see Figure 9).

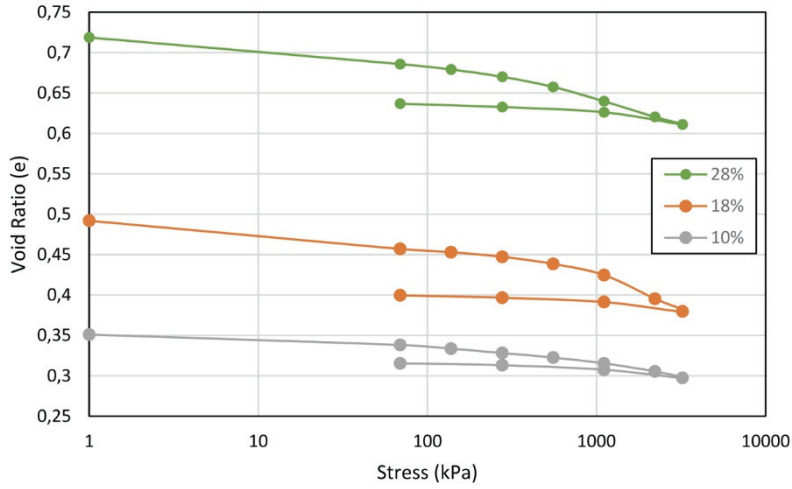

Figure 9 - Compression curves for the unsaturated oedometric compression tests

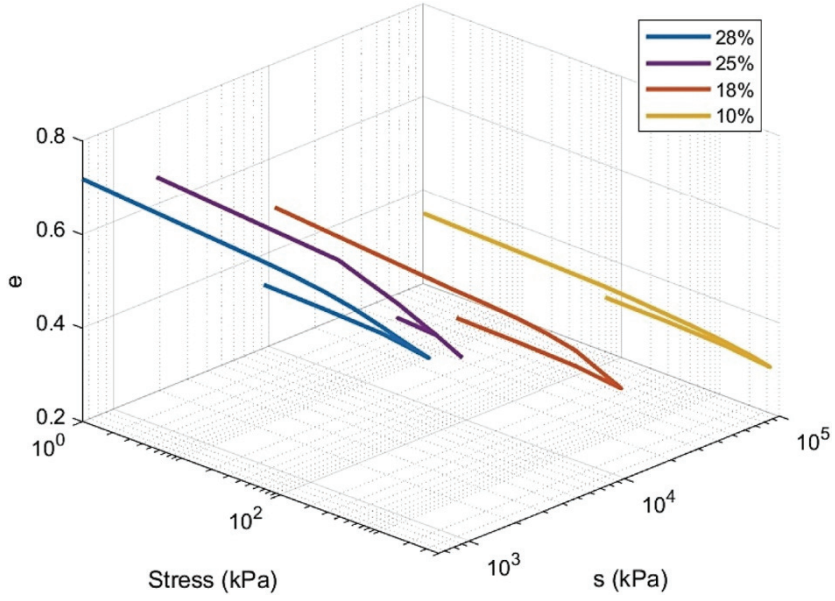

Figure 10 - Compression curves for saturated and unsaturated oedometric compression

From the above Figure, it can be seen that all samples had different void ratios at the beginning of the tests, even though they all belonged to the same sample. It is important to note here that these varying void ratios are due to the drying process carried out prior to starting the tests.

The results of the unsaturated oedometric compression tests were also plotted in an e-log σ-s space. The values of suction were determined from the results of the SWRC curve fitting. This soaked oedometric compression curve was also incorporated into this plot (see Figure 10). It can be seen that this specimen also contained suction-despite being soaked-as it only reached a moisture content of 25%.

5.4. Unsaturated UU Triaxial Tests

Unsaturated UU triaxial tests were carried out on specimens at three values of gravimetric moisture contents-9%, 19% and 29%--and two confining pressures-100 and 400 kPa. The values of the moisture contents were selected such that there was one value with very high suctions below the shrinkage limit (9%), one value where suction was close to zero (29%) and one intermediate value (19%). These values of confining pressure were kept same as that of the saturated triaxial tests in order to make comparisons easier. In this way, a total of six tests were planned but only five could be carried out due to limited specimen availability. At 29% moisture content, only one test was carried out at 100 kPa.

Specimens were trimmed and dried to the required moisture content in intervals such that shrinkage cracks could be minimized. The tests were then carried out by omitting the saturation and consolidation phases. An initial pressure equal to the confining pressure was

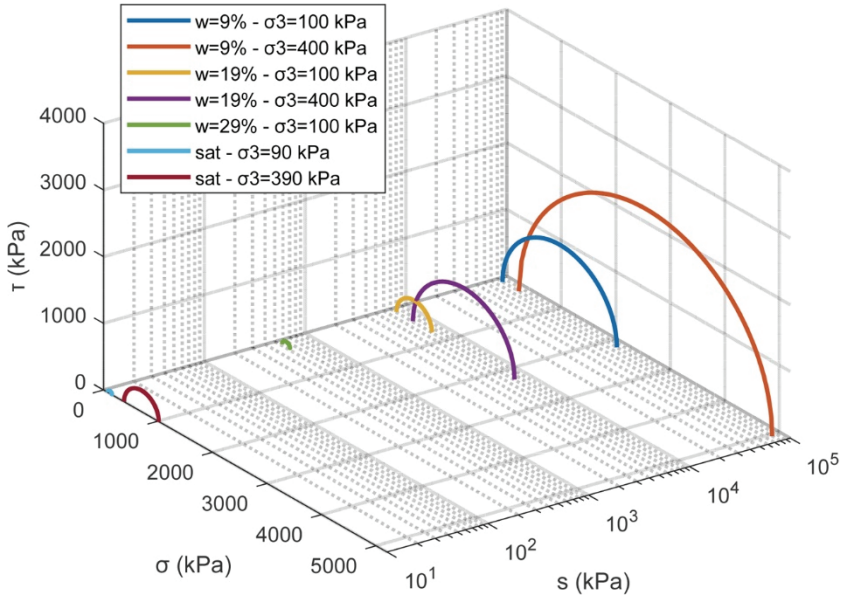

Figure 11 - Results of the UU triaxial tests in a σ-τ-log s space

applied and then the specimen was sheared at a strain rate of 1% per minute, which was selected in accordance with ASTM D2850-15. Air drainage was permitted throughout the test by opening the drainage valve to the atmosphere. Inside the test setup, the movement of water out of the specimen was restricted using dry filter paper and dry porous stones at the top and bottom. Furthermore, filter strips were not used in order to make it more difficult for the water to drain out of the specimen.

Mohr's circles for all unsaturated tests were plotted in a σ-τ-log s space (see Figure 11). Once again, values of suction were taken from the results of the SWRC curve fitting. Results of the CD triaxial tests were also incorporated in this Figure by converting the effective stress in the CD triaxial tests into total stress. A hypothetical suction of 10 kPa was assumed. This is low enough that total saturation and, therefore, the validity of the effective stress principle is assured. This had to be done for the sake of plotting this diagram on a logarithmic stress scale.

Failure envelopes for saturated (32%), 9% and 19% moisture content tests are also plotted in a two-dimensional space in order to better visualize their changes with change in moisture content (see Figure 12). As expected, cohesion increases when moisture content decreases. However, friction angle also seems to increase (see Table 2).

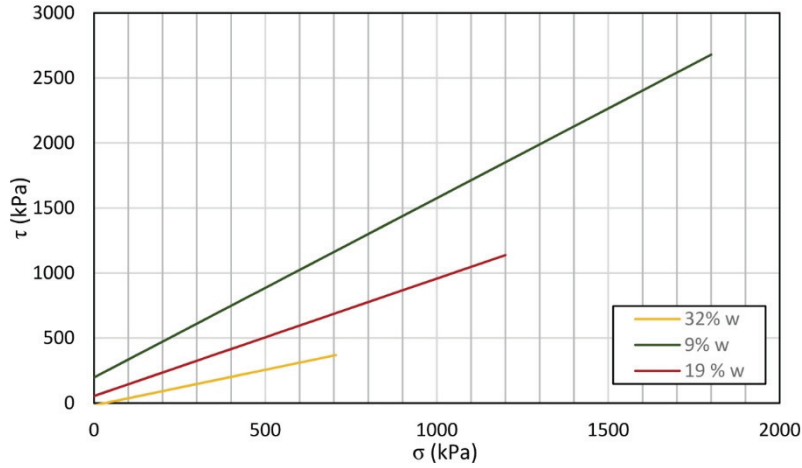

Figure 12 - Strength envelopes for various moisture contents

Table 2 - Values of total cohesion and friction angle for each strength envelope in Figure 12

Moisture Content	c	ϕ
Saturated (30.9 – 32.8%)	-18.25	28.72
19 %	53.89	42.08
9 %	196.39	54.05

The strength envelopes of all the Mohr's circles were then connected into a single plane, as per [10], using the equation:

$$\tau = c' + \sigma' tan\phi' + s tan\phi_b \quad (10)$$

This was done by first fitting the top points of the Mohr's circles were also fit to the equation of a plane:

$$\frac{\sigma_1 - \sigma_3}{2} = a_0 + a_1 \frac{\sigma_1 + \sigma_3}{2} + a_2 s \quad (11)$$

Seven sets of values of $\frac{\sigma_1 - \sigma_3}{2}$, $\frac{\sigma_1 + \sigma_3}{2}$ and s corresponding to the peaks of the Mohr's circles were obtained. Equation 11 was fit to that data using optimization and values of a_0, a_1 and a_2 were obtained as -87.9 kPa, 0.75353 and 0.00397.

However, the negative value of a_0 would have further led to a negative value of cohesion. Therefore optimization was repeated whilst constraining the value of a_0 as 0. This time, the values of a_1 and a_2 were obtained as 0.6911 and 0.0043.

Using the values of a_0, a_1 and a_2, the constants in Equation 10 were calculated and the values of c', ϕ' and ϕ_b were obtained as 0 kPa, 43.7° and 0.249°. The value of ϕ_b obtained here appears to be lower than commonly seen in literature. However, it is important to note here that the values of suction in this soil are very high, therefore, the product of suction and tan(ϕ_b) would yield a normal value.

Mohr's circles of the seven tests are plotted in 3D, together with the strength envelope defined by these parameters in Figure 13.

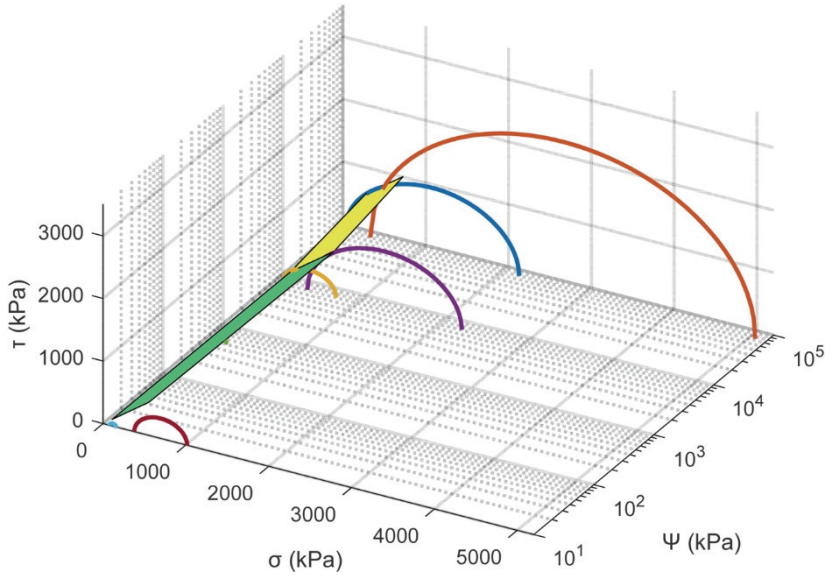

Figure 13 - Surface plot connecting the strength envelopes obtained from the results of the second optimization trial (c' = 0) in a σ-τ-log s space

The testing program was carried out as detailed in the above section. Saturated and unsaturated properties of the sample were obtained. Valuable insights were gained regarding the strength parameters and behaviour of this sample. However, in order to paint an even better picture of the behaviour of any soil under various loadings, soil models are necessary. These models can be calibrated using the properties of a certain soil and then used to predict its behaviour.

Therefore, the results of these experiments were used to carry out such a calibration. The Barcelona Basic Model (BBM) was used for this purpose as it is one of the first and most notable unsaturated soil model. An attempt was made at modelling the unsaturated behaviour of this sample of Ankara Clay when subjected to shear and compressive loading.

6. CALIBRATION OF BARCELONA BASIC MODEL

6.1. Determination of Parameters

The results of the experimental campaign were also used to calibrate the BBM. The calibration procedure as outlined in [2] was followed. Values of certain parameters such as κ, M, λ(0) and k were determined from the results of the saturated and unsaturated triaxial and oedometric compression tests.

As mentioned earlier, the value of M was determined from the slope of the critical state line as 1.14. The value of κ was determined using the slopes of oedometric recompression lines. Firstly, the value of the friction angle was determined as 28.72, as mentioned earlier. This was used in conjunction with the following formula to calculate the value of K_0 [11]:

$$K_0 = 1 - sin\phi * \sqrt{OCR} \tag{13}$$

Using the above equation, the value of K_0 was calculated as 0.088 It is also important to note here that the value of friction angle used here corresponds to the saturated friction angle. This is because this formula was developed for saturated soils.

The values of the slopes of the oedometric recompression lines were then converted to mean stress using the formula:

$$\kappa = C_r \log\left(\frac{1+2K_0}{3}\right) \tag{14}$$

where C_r is the slope of the recompression lines. Finally, the average of all values of κ was calculated as 0.003.

λ(0) is simply the slope of the saturated virgin compression line which was determined earlier as 0.092.

k parameter is used to quantify the contribution of suction to the cohesion. To calculate this, the experimental values of apparent cohesion were determined for each of the UU triaxial tests as follows:

$$c = \frac{\frac{\sigma_{dev}}{2}(1-sin\,\phi)-\sigma_c sin\phi}{cos\phi} \tag{15}$$

where c is the total cohesion, σ_{dev} is the deviator stress, σ_c is the net confining pressure and ϕ is the friction angle.

BBM expresses the contribution of soil suction to the cohesion i.e. the apparent tensile strength (ATS) as a product of the k parameter and suction and can mathematically be expressed as:

$$ATS = k * s = \frac{c}{\tan(\phi)} \tag{16}$$

Therefore, the value of k can be calculated by plotting a linear relationship between p_s and suction as shown below:

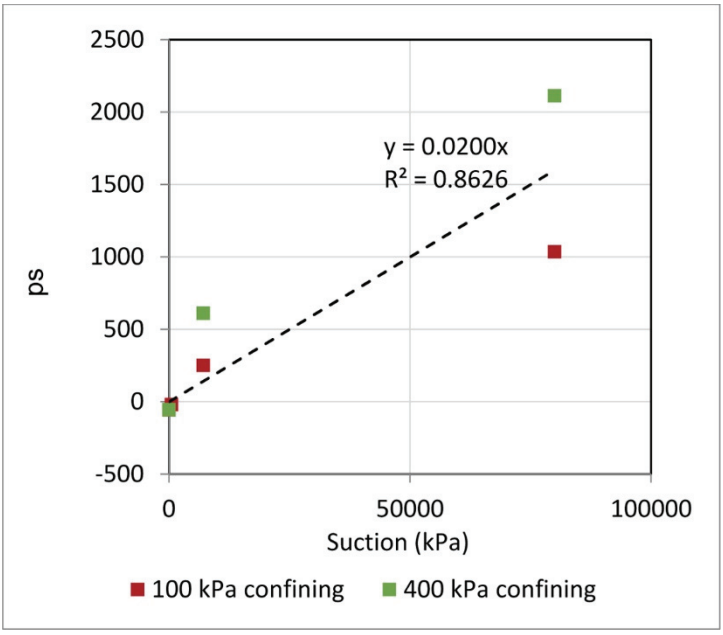

Figure 14 - Linear relationship between ATS and suction

As can be seen in Figure 14, the value of k was determined as 0.0200. It is important to note here that some studies have also attempted to model this ATS as a nonlinear relationship [12].

The value of r was determined as:

$$r = \frac{C_{r_{s\to\infty}}}{C_{r_{sat}}} \tag{17}$$

where $C_{r_{s\to\infty}}$ is the slope of the recompression line at the highest suction and $C_{r_{sat}}$ is its saturated counterpart.

For the value of shear modulus (G), individual values were calculated from the stress-strain graphs of all of the CD and UU triaxial results (see Figure 15). Arithematic mean of G values at which moisture content was calculated and used for calibration in the triaxial and oedometer tests (see Table 3).

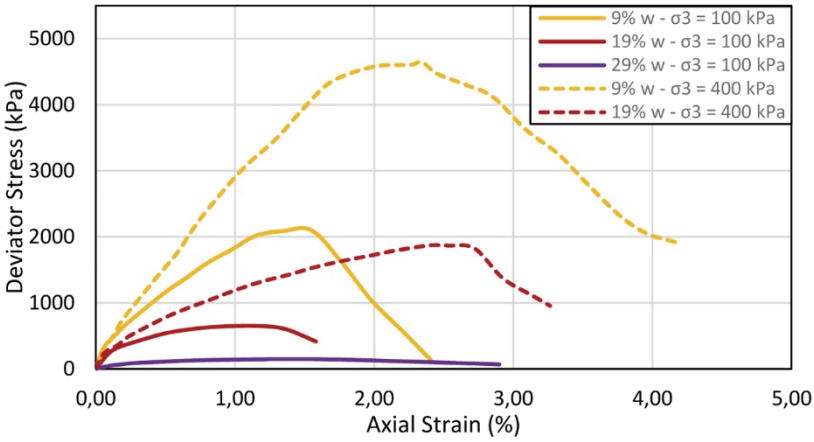

Figure 15 - Deviator stress versus axial strain plots for UU triaxial tests

Table 3 - Values of shear modulus at different moisture contents

Moisture Content (%)	Average Value of G (MPa)
28-29	5
18-19	15
9-10	50

Values of a, n, m, θ_{sat}, and θ_{res} were determined during the SWRC curve fitting and kept the same in this calibration. Table 4 details the values of BBM parameters which were calculated from the results of different types of experiments.

These calculated values, when calibrated onto the results of UU triaxial tests, produced a good fit. However, for the calibration of the oedometer tests, values of certain parameters such as $\lambda(0)$, κ, r, M and k had to modified to be produce a good fit. The initial calculated values of all these parameters were obtained from the results of the saturated and unsaturated oedometric compression tests. However, those calculated values, when input into the BBM formulations, did not accurately model the soil behavior. Therefore, they were changed in order to produce a good fit with minimal error. Deviance between experimental and model values was minimzed using the method of least squares and a final relative error of 3.8% was calculated.

Furthermore, during the calibration procedure, values of certain parameters were manually selected such that the results of the model matched those of the experiments as closely as possible and errors were minimized. These included:

- p_c, which represents the stress point where plastic deformations commence
- p_0^*, which represents the initial reference stress and defines the initial position of the yield surface. This value is individually adjusted for each test since initial conditions (suction and confining pressure) were different in each
- β, which controls the rate of increase in stiffness in virgin states with suction

Table 4 - Values of calculated parameters for UU triaxial and oedometer tests

Parameter	Value for UU triaxial tests	Value for oedometer tests
κ	3×10^{-3}	9.0×10^{-3}
r	0.422	0.570
M	1.140	1.100
$\lambda(0)$	0.092	0.020
k	0.019	0.020
a	38000	38000
n	0.550	0.550
m	1.050	1.050
θ_{sat}	0.456	0.456
θ_{res}	0.047	0.047

6.2. Results of calibration

Finally, optimization was done and the results of the BBM calibration were plotted alongside experimental results (see Figures 16 and 17.

As can be seen in Figure 16, the results of the BBM calibration are better equipped to model low to moderate strains and do not accurately capture the post-yield behavior . It is also noteworthy that this deviation appears to be more prominent in soils with higher suction. This indicates that BBM cannot accurately capture the brittle behavior of Ankara Clay at high suctions and this can likely be attributed to the fissure formation which Ankara Clay exhibits at these high suctions.

From Figure 17, it appears that the BBM is a good fit for modelling 1-D compression. However, the values of input parameters were different for the UU triaxial and the oedometer tests for the same soil sample. Therefore, we conclude that one set of BBM parameters cannot accurately model the entire behaviour of Ankara Clay.

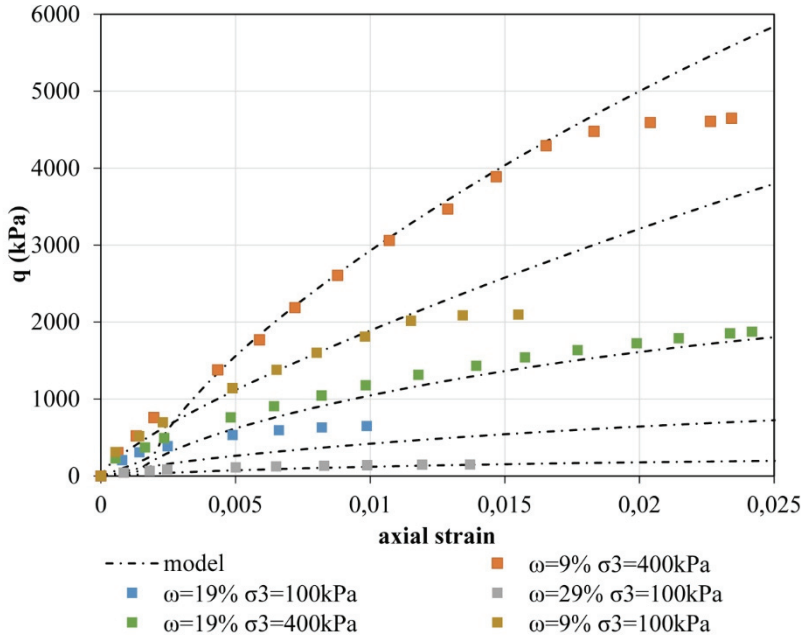

Figure 16 - Results of calibration for UU triaxial tests

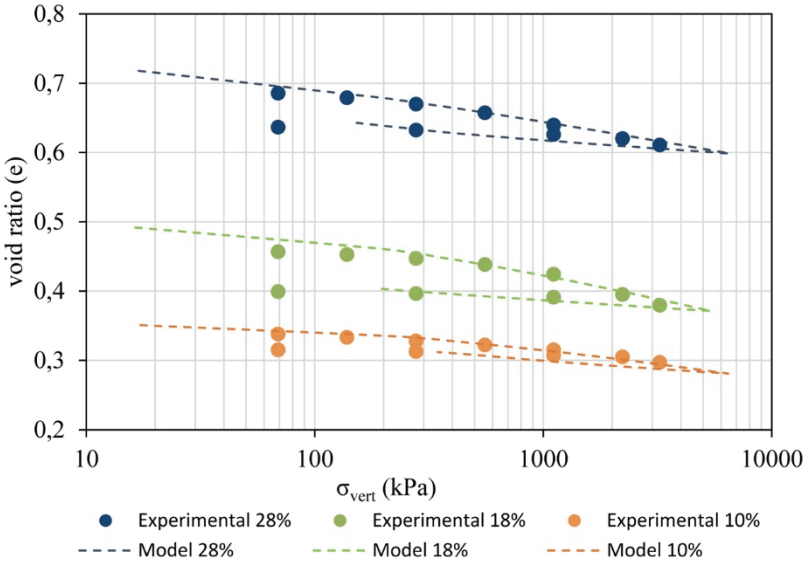

Figure 17 - Results of calibration for oedometric compression tests

From the results of this calibration exercise, it can be concluded that BBM is not an appropriate model for stiff high-plasticity clays like Ankara Clay. The main reason for this is that it cannot accurately capture the brittle behaviour that Ankara Clay exhibits at high suctions. This is likely due to the formation of fissures at high suctions, due to the expansive nature of Ankara Clay and the unusually high amounts of suction that it can have. These fissures act as predetermined failure planes during shearing and compressive loading, thus altering the behaviour of the soil.

However, it is also important to note here that, Ankara Clay in the field is not likely to have, suctions high enough to induce this brittle behaviour. In Figure 16, it can be seen that the brittle behaviour is exhibited at 9% moisture content, which corresponds to a suction of 80000 kPa according to the SWRC. Practically, it is unlikely that local soils in the region will experience these levels of suction as the samples had a natural water content of around 30% even though they were taken from shallow depths high above the ground water level following the hottest and driest season of the year.

7. CONCLUSION

In this study, an attempt was made to calibrate the BBM for intact samples of Ankara Clay. However, the results of the calibration demonstrate that BBM is not suitable to model the behaviour of Ankara Clay or other similar high-plasticity expansive fissured clays at high suctions. This can be deduced from the fact that two separate sets of parameters were required for the triaxial and oedometer calibrations for the same soil sample. Furthermore, at high strains and close to yielding, the BBM model appears to deviate from the experimental results. It is also important to note here that this deviation is more prominent at high suctions, when fissures have likely developed in the soil. Therefore, other constitutive models developed for unsaturated soils should be explored to model the in-situ behaviour of Ankara Clay.

The findings of this study are also supported by exisitng literature which indicates that BBM is good at modelling low-to-medium plasticity clays and silty soils [2] [1] [13]. Researchers who have attempted to use BBM to model soils which exhibit problematic or unsual behaviour have often reached similar findings of BBM being unsuitable for use to emulate soil behaviour [14] [15].

However, it is also important to keep in mind that the behaviour of Ankara Clay has large spatial variability, especially when dealing with undisturbed samples. Therefore, the authors recommend further studies be carried out by replicating this methodology but using samples of Ankara Clay from different sites. Furthermore, the imperfections that are inherently and unavoidably present in undisturbed samples of Ankara Clay-such as gravel, fissures or calcareous concretions-are also likely to impact the results of this calibration.

List of Symbols

c	Total cohesion
c’	Effective cohesion

C_r	Recompression index
$C_{r_{s\to\infty}}$	Slope of the recompression line at the highest suction
$C_{r_{sat}}$	Slope of saturated recompression line
N(s)	specific volume corresponding to the extension of the virgin compression line
N(0)	specific volume at reference stress for the virgin saturated compression line
p	net stress
p_{atm}	atmospheric pressure
p_c	reference stress
p_0^*	pre-consolidation stress for saturated condition
r	ratio of the asymptotic value of compression index as suction tends to infinity to saturated compression index λ(0)
s	matric suction
s_{aev}	air-entry value of the suction
α	parameter used to define associated or non-associated flow rule
β	Parameter controlling the rate of increase of soil stiffness with suction
θ	volumetric water content
θ_{res}	residual volumetric water content
θ_{sat}	saturated volumetric water content
κ_s	slope of the elastic compression line due to suction change
λ(0)	slope of the saturated virgin compression line
σ_{dev}	deviator stress
σ_c	net confining pressure
ϕ	friction angle

References

[1] E. E. Alonso, A. Gens, and A. Josa, "A constitutive model for partially saturated soils," *Géotechnique*, vol. 40, no. 3, pp. 405–430, Sep. 1990, doi: 10.1680/geot.1990.40.3.405.

[2] M. B. Kenanoğlu, "Determination of Unsaturated Soil Properties from Simplified Experimental Procedures," Middle East Technical University, Ankara, Turkey, 2023.

[3] R. A. Naghadeh, "Hydro-Mechanical Behavior of Unsaturated Specimens Isotropically Reconstituted from Slurry and Compacted Specimens," Middle East Technical University, Turkey, 2016.

[4] F. Tunçdemir and M. U. Ergun, "A Laboratory Study into Fracture Grouting of Fissured Ankara Clay," in *Innovations in Grouting and Soil Improvement*, Austin, Texas, United States: American Society of Civil Engineers, Oct. 2005, pp. 1–12. doi: 10.1061/40783(162)16.

[5] Z. A. Erguler and R. Ulusay, "Engineering characteristics and environmental impacts of the expansive Ankara Clay, and swelling maps for SW and central parts of the Ankara (Turkey) metropolitan area," *Environ. Geol.*, vol. 44, no. 8, pp. 979–992, Nov. 2003, doi: 10.1007/s00254-003-0841-y.

[6] M. Fredlund, G. W. Wilson, and D. Fredlund, "Representation and estimation of the shrinkage curve," vol. 1, pp. 145–149, Mar. 2002.

[7] M. Basharat and N. K. Toker, "Utility of Temperature Control on Suction Application by Vapour Equilibrium Technique," presented at the 8th Asia-Pacific Conference on Unsaturated Soils, Melbourne, 2024.

[8] M. Th. Van Genuchten, "A closed-form equation for predicting the hydraulic conductivity of unsaturated soils," *Soil Sci. Soc. Am. J.*, pp. 892–898, 1980.

[9] A. W. Bishop and D. J. Henkel, *The Measurement of Soil Properties in the Triaxial Test*. Edward Arnold, 1964.

[10] D. G. Fredlund and N. R. Morgenstern, "Stress State Variables for Unsaturated Soils," *J. Geotech. Eng. Div.*, vol. 103, no. 5, pp. 447–466, May 1977, doi: 10.1061/AJGEB6.0000423.

[11] J. Jaky, "The coefficient of earth pressure at rest," *J. Soc. Hung. Archit. Eng.*, 1944, Accessed: Feb. 11, 2025. [Online]. Available: https://cir.nii.ac.jp/crid/1571135650251603584

[12] L. R. Hoyos and D. D. Pérez-Ruiz, "A Refined Approach to Barcelona Basic Model Using the Apparent Tensile Strength Concept," in *Unsaturated Soils: Research and Applications: Volume 2*, 2012.

[13] R. Quevedo, C. Romanel, and D. Roehl, "Numerical modeling of unsaturated soil behavior considering different constitutive models," *MATEC Web Conf.*, vol. 337, p. 02007, 2021, doi: 10.1051/matecconf/202133702007.

[14] J. C. B. Benatti, R. A. Rodrigues, and M. G. Miguel, "Aspects of Mechanical Behavior and Modeling of a Tropical Unsaturated Soil," *Geotech. Geol. Eng.*, vol. 31, no. 5, pp. 1569–1585, Oct. 2013, doi: 10.1007/s10706-013-9682-y.

[15] M. Aukenthaler, "The frozen & unfrozen Barcelona Basic Model," PhD Thesis, TU Delft, 2016. Accessed: Feb. 11, 2025. [Online]. Available: https://repository.tudelft.nl/record/uuid:95917a12-00dd-4ace-b86d-048833c510df